

**Analytic description of dipole-bound anion photodetachment**

V. E. Chernov, A. V. Dolgikh, and B. A. Zon\*

*Voronezh State University, 1 University Sq., Voronezh, 394006, Russia*

(Received 24 May 2005; published 2 November 2005)

An analytical model for a dipole-bound anion (DBA) is proposed based on the exactly solvable three-dimensional Schrödinger equation for the excess electron bound by dipole potential of the parent neutral molecule (NM) in the Born–Oppenheimer approximation. The model gives reasonable analytical approximation for the dependence of the DBA binding energy on the NM dipole moment previously found numerically by many authors. The cross section of one-photon photodetachment of DBA is calculated in explicit analytical form. In the limit of high photon frequency,  $\omega$ , the calculated cross-section displays  $\sim \omega^{-2}$  behavior, which agrees perfectly with the experimental data [Bailey *et al.*, *J. Chem. Phys.* **104**, 6976 (1996)]. At the threshold, the cross section demonstrates Gailitis–Damburg oscillations. Numerical dependence is provided for the maximal value of the cross section as a function of the NM dipole moment and the binding energy of the excess electron.

DOI: 10.1103/PhysRevA.72.052701

PACS number(s): 33.80.Eh, 33.15.Ry

**I. INTRODUCTION**

Considerable attention is presently paid to the so-called dipole-bound anions (DBA), i.e., molecular negative ions in which the excess electron is bounded to the neutral molecule (NM) due to its dipole moment [1,2]. As early as in 1947, Fermi and Teller [3] and, later, Wightman [4] in their analysis of meson capture by hydrogen atoms noted that a fixed point dipole  $d > 1.625$  D (1 Debye  $\approx 0.393$  a.u.) can bind an electron to infinitely many bound states. A number of subsequent studies taking into account the finite dipole effects [5–8], presence of a short-range repulsive core potential [9,10], rotational excitation [11–13], polarization [14–17], and quadrupolar [14,15,18] interaction yield the critical dipole moment 2–2.5 D required to form DBAs of common molecules [1,19].

DBAs for experimental studies are created, for instance, by proton [20,21] and  $\text{H}_2^+$  [22] abstraction reactions, hot cathode electric discharge [23–25], free electron attachment under high-pressure nozzle expansion conditions, [26–29] and charge transfer from Rydberg atoms [19,30,31]. Recently, a new method of laser stimulated radiative attachment has been proposed in Ref. [32]. The created DBAs are investigated, e.g., by photoelectron spectroscopy [26–29,31,33].

Large-scale *ab initio* calculations (see, for instance, [[29,34–42] and references therein) of a DBA structure were used to study the effects of correlation, orbital relaxation, dispersion, and charge-transfer interaction. However, despite the increasing accuracy of such many-electron calculations, simplified one-electron local model potentials have still been proving their efficiency and suitability for large-scale computer simulations, as well as for other analytical theories [43] and references therein).

While the structure of DBA is being studied very actively, until recently, there have been no theoretical estimates of the cross sections reported for photodetachment (PD) from DBA

[44–46]. From the theoretical point of view, the threshold behavior of such cross sections is an interesting manifestation of different interactions felt by an outgoing photoelectron [47]. In fact, the dipole potential of NM makes DBA an intermediate case between the neutral atoms and atomic anions. In the former case, the Coulomb interaction causes the constant cross section value at the threshold, while in the latter case the short-range (such as polarization or quadrupole) potentials do not affect the leading term of the well-known Wigner threshold law for the PD cross section:

$$\sigma \propto k^{2l+1} \text{ or } \sigma \propto (\hbar\omega - E_b)^{l+1/2}, \quad (1)$$

where  $k$  and  $l$  are linear and angular momenta of the outgoing electron,  $\omega$  is the photon frequency, and  $E_b$  is the binding (threshold) energy.

Anomalous threshold behavior of PD from DBA was predicted theoretically to be caused by the dipole potential which breaks the spherical symmetry resulting in the noninteger  $l$  value in expression (1) [48,49]. Moreover, for above-critical dipole moment, the threshold behavior of the PD cross-section is closer to the Coulomb than to the short-range case: At  $\hbar\omega \rightarrow E_b$ , it is almost constant with weak superimposed oscillations with  $\omega$ . Such oscillations were first predicted for electrons scattered from hydrogen atom excited states [50]. They are due to the constant dipole moment of excited states of the nonrelativistic hydrogen atom, as well as the linear Stark effect. Similar oscillations were discussed for single and double one-photon [51] and two-photon [52] PD from the hydrogen anion and also for electron scattering on polar molecules [53] (see also Ref. [47]).

Experiments for the dipole effects in the threshold behavior of a PD cross section have been actively discussed [54–57]. Nevertheless, there are other experimental aspects of PD measurements on DBA which require theoretical description. The frequency dependence of PD was measured in Ref. [33]. DBA lifetimes measured in Ref. [45] are attributed to PD induced by background thermal black-body radiation.

Recently, [46] one-electron calculations of PD from DBA were performed in the framework of the Drude oscillator

\*Electronic address: zon@niif.vsu.ru

model, which was used as a pseudopotential of NM. In this work, we consider a DBA as an electron moving in a point dipole potential. Below, we develop an analytical theory explaining some features of frequency-dependent DBA PD. While most experimental photoelectron spectra are recorded at a constant photon frequency  $\omega$ , Ref. [33] reports the photodetachment rate  $\propto \omega^{-2}$  for high  $\omega$ . Such behavior is different from the PD cross section  $\propto \omega^{-7/2}$  in atoms [58] and  $\propto \omega^{-3/2}$  in atomic negative ions [59], and can be explained using the proposed analytical technique. Our model also implies the above-mentioned oscillatory behavior of the cross-section near threshold.

In Sec. II, we start from the full Hamiltonian which includes the interaction of a rotating NM with the excess electron and briefly describe separation of the angular variables in two opposite limiting cases; Born-Oppenheimer approximation (BOA) (Sec. II A) and inverse BOA (IBOA) (Sec. II B). The radial wave functions are constructed in Sec. III with separate consideration of bound states (Sec. III A) and scattering states with necessary asymptotics (Sec. III B). The general expressions for the PD cross section are given in Sec. IV.

## II. GENERAL FORMALISM AND ANGULAR FUNCTIONS

We assume that the NM remains in one of its vibrational states and its rotational state is determined by its angular momentum,  $j$ . We choose a NM-fixed reference frame  $(\xi, \eta, \zeta)$  with the  $\zeta$ -axis directed along the NM dipole moment  $\mathbf{d}$ , which is considered to be a point dipole [60]. Then, the Hamiltonian of the excess electron moving in the field of the rotating NM is

$$\hat{H} = \hat{H}_{\text{rot}} + T_e + V(r, \cos \vartheta). \quad (2)$$

The rotational Hamiltonian,

$$\hat{H}_{\text{rot}} = b_\xi \hat{j}_\xi^2 + b_\eta \hat{j}_\eta^2 + b_\zeta \hat{j}_\zeta^2, \quad (3)$$

includes the rotational constants  $b_\xi, b_\eta$  and  $b_\zeta$ . For a symmetric-top NM, we have  $b_\xi = b_\eta$  and the expression (3) is reduced to

$$\hat{H}_{\text{rot}} = b_\xi \hat{j}^2 + (b_\xi - b_\zeta) \hat{j}_\zeta^2. \quad (4)$$

The kinetic energy,

$$T_e = \frac{\hbar^2}{2m_e r^2} \frac{d}{dr} \left( r^2 \frac{d}{dr} \right) + \frac{\hbar^2 \hat{\mathbf{I}}^2}{2m_e r^2}, \quad (5)$$

of the excess electron and its interaction,

$$V(r, \cos \vartheta) = -\frac{\beta \cos \vartheta}{r^2}, \quad (6)$$

with the rotating NM includes the electron radius vector,  $\mathbf{r}$ , whose direction is determined by the spherical angles  $(\vartheta, \varphi)$  in the molecule-fixed frame. The dimensionless dipole moment  $\beta = 2m_e |e| d / \hbar^2 = 0.786 d(D), e$  and  $m_e$  are the electron charge and mass, respectively.

The solution of Schrödinger equation with the Hamiltonian (2) can be found as a sum over the channels corresponding to different NM states:

$$\Psi = \sum_{J_c l} R_{J_c l}(r) \Phi_{J_c l}^{JM}, \quad (7)$$

$$\Phi_{J_c l}^{JM} = \sum_{M_c m} C_{J_c M_c l m}^{JM} \mathcal{B}_{K_c M_c}^{J_c}(\Theta) Y_{lm}(\theta, \phi), \quad (8)$$

where the eigenfunctions of the rotational NM Hamiltonian (3)

$$\mathcal{B}_{K_c M_c}^{J_c}(\Theta) = \sqrt{\frac{2J_c + 1}{8\pi^2}} \sum_{\Omega_c} b_{K_c \Omega_c} D_{M_c \Omega_c}^{J_c*}(\Theta), \quad (9)$$

are expressed as linear combinations of the Wigner  $D$  functions which are eigenfunctions of the symmetric-top rotational Hamiltonian (3); they depend on the corresponding Euler angles,  $\Theta$ . Since the  $\zeta$ -projection,  $\Omega_c$ , of the NM angular momentum,  $J_c$ , is not conserved for an asymmetric-top NM, the corresponding wave function (9) contains a sum over  $\Omega_c$  and depends on the quantum number  $K_c$ , which can be obtained by diagonalization of the Hamiltonian (3). For symmetric-top-type-NM, one has  $b_{K_c \Omega_c} = \delta_{K_c \Omega_c}$ .

The spherical functions  $Y_{lm}$  depend on the angles  $(\theta, \phi)$  of the electron in the space-fixed frame  $(x, y, z)$ . Due to the sum with over Clebsch–Gordan coefficients  $C$  with the  $z$ -projections,  $M_c$  and  $m$  of the NM and electron angular momenta,  $J_c$  and  $l$ , correspondingly, the angular functions  $\Phi_{J_c l}^{JM}$  describe the states with total DBA angular momentum,  $J$ , and its  $z$ -projection,  $M$ . The sum over the electron orbital momentum,  $l$ , (so called  $l$  mixing) is caused by nonspherical symmetry of the MN potential  $V$  in Eq. (2). However for a point dipole potential (6), one has  $R_{J_c l}(r) \equiv \mathcal{A}_{\eta J_c l} R_{\eta J_c}(r)$  with the  $l$ -mixing coefficients,  $\mathcal{A}_{\eta J_c l}$ , independent of  $r$  [60]. The quantum number  $\eta$  arises instead of the angular momentum,  $l$ , due to this mixing, see Eq. (14) below.

### A. Born-oppenheimer approximation

Wavefunction (7) in the previous section has a quite complicated analytical form. More simple expressions for it can be obtained in two limiting cases. The first case, BOA, takes place when the NM rotation is slow compared to the electron motion. Quantitatively, the difference between the energy levels of the NM states with neighboring  $J_c$  values in BOA is small compared with the difference between the electron levels, so that we can consider the radial function  $R_{\eta J_c}(r) \equiv R_\eta(r)$  to be independent of  $J_c$ . It is convenient to transfer to the molecule-fixed frame according to

$$Y_{lm}(\theta, \phi) = \sum_{\mu} D_{m\mu}^{l*}(\Theta) Y_{l\mu}(\vartheta, \varphi). \quad (10)$$

Since the  $\zeta$ -projection,  $\lambda$ , of the electron angular momentum is conserved in BOA, one can choose the  $\mathcal{A}_{\eta J_c l}$  coefficients, so that only one term with  $\mu = \lambda$  would remain in the sum of the expression (10) after its substitution into the Eq. (7). Indeed, such an operation is well known as the transition from the Hund's  $d$  wave functions (8) to the Hund's  $d$  wave functions [see Eq. (12) below], and plays an important role in multichannel quantum defect theory [61]. Assuming

$$A_{\eta J l} = (-1)^{l+\lambda} C_{l, -\lambda; J, \lambda+\Omega_c}^{J, \Omega_c} a_{\eta l}^{(\lambda)}. \quad (11)$$

and using properties of Clebsch–Gordan coefficients and Wigner functions, we obtain

$$\Psi = \mathcal{D}_{K_c M \lambda}^J(\Theta) R_{\eta}(r) \mathcal{Z}_{\eta \lambda}(\vartheta, \varphi), \quad (12)$$

$$\mathcal{D}_{K_c M \lambda}^J(\Theta) = \sqrt{\frac{2J+1}{8\pi^2}} \sum_{\Omega_c} b_{K_c \Omega_c} D_{M \Omega_c + \lambda}^{J*}(\Theta),$$

$$\mathcal{Z}_{\eta \lambda}(\vartheta, \varphi) = \sum_l a_{\eta l}^{(\lambda)} Y_{l \lambda}(\vartheta, \varphi), \quad (13)$$

where the BOA dipole-spherical angular functions  $\mathcal{Z}_{\eta \lambda}$  satisfy the equation

$$(-\hat{I}^2 + \beta \cos \vartheta) \mathcal{Z}_{\eta \lambda} = \eta \mathcal{Z}_{\eta \lambda}. \quad (14)$$

Together with the  $l$ -mixing coefficients,  $a_{\eta l}^{(\lambda)}$ , the dipole-spherical functions  $\mathcal{Z}_{\eta \lambda}$  depend on the eigenvalue  $\eta$  of the operator (14), and  $\eta \rightarrow l(l+1)$ ,  $l=0, 1, \dots$  for  $d \rightarrow 0$ . This three-diagonal eigenvalue problem was studied in numerous works. The functions  $\mathcal{Z}_{\eta \lambda}$  were used as early as in Debye's works on the Stark effect for polar molecules [62]. The same functions were used in the analysis of the critical binding dipole moment in DBA [7] without studying the radial functions. In Refs. [63,64] these dipole-spherical functions were applied to Rydberg states in polar molecules. Recently, these functions were used in calculations of oscillator strengths in excimer molecules in Refs. [65,66] and in strong-field PD of atomic anions [67]. Some properties of  $a_{\eta l}^{(\lambda)}$  coefficients and  $\mathcal{Z}_{\eta \lambda}$  functions, including their plots, are presented in Refs. [65,67].

Note that for a symmetric-top NM, the wave functions  $\mathcal{D}$  are reduced to the Wigner  $D$  functions and the Hund's case  $b$  (or, in other words, BOA) functions (12) take the form

$$\Psi = \sqrt{\frac{2J+1}{8\pi^2}} D_{M \Omega}^{J*} R_{\eta} \mathcal{Z}_{\eta \lambda} \quad (15)$$

with the conserving  $\zeta$ -projection,  $\Omega = \Omega_c + \lambda$ , of the total DBA angular momentum,  $J$ .

### B. Inverse Born–Oppenheimer approximation

While BOA is good for calculations of ground state binding energy of DBA, for some phenomena, such as rotational autodetachment [22,68,69], non-BOA effects are important. The opposite limiting case, IBOA, corresponds to Hund's case  $d$  and it is fulfilled when the excess electron moves far away ( $r \sim 10..100 \text{ \AA}$ ) from NM, and its motion can be considered slow compared to the NM rotation (not to vibration, see the beginning of Sec. II):

$$E_b \lesssim 2bj, \quad (16)$$

where  $b$  is of order of NM's rotational constants. For a very weakly bound (e.g., to an excited state) DBA with  $E_b \sim 10 \text{ cm}^{-1}$ , and a heavy NM ( $b \sim 10 \text{ cm}^{-1}$ ) in high-momentum ( $j \sim 10$ ) state, condition (16) could take place.

Thus, in IBOA, only one term remains in Eq. (7) corresponding to the conserving NM angular momentum  $j$  [60]. Wave functions similar to  $\Phi_{J l}^{JM}$  (8), without  $l$  mixing, were used, e. g., in description of dipole coupling channels [49] and rotational autodetachment of DBA [68,69].

For the point-dipole potential (6) in both limiting cases, BOA and IBOA, the expression in Eq. (7) is effectively reduced to a single-channel radial function multiplied by the appropriate angular function. The latter has a simpler form in the BOA case, so all of the following results—which are not so sensitive to the dependence of the electron wave function on the angular variables—will be formulated for the BOA case.

### III. RADIAL FUNCTIONS AND ENERGY SPECTRUM

The radial functions satisfy

$$\frac{1}{r^2} \frac{d}{dr} \left( r^2 \frac{dR}{dr} \right) - \frac{\eta}{r^2} R + \frac{2m_e E}{\hbar^2} R = 0, \quad (17)$$

for both BOA and IBOA; the difference between them is included in  $\eta$ .

#### A. Bound states

Wave functions  $R_{\kappa \eta}(r)$  of bound states are solutions to Eq. (17) for  $E = -1/2 \hbar^2 \kappa^2 / m_e$  with decreasing asymptotics  $R_{\kappa \eta}(r) \rightarrow 0$  at  $r \rightarrow \infty$ . Therefore, to a normalization factor,  $N_{\kappa \eta}$ , they equal McDonald functions [[70], Vol. 2]:

$$R_{\kappa \eta}(r) = \frac{N_{\kappa \eta}}{\sqrt{r}} K_{\rho}(\kappa r) \underset{r \rightarrow \infty}{\sim} N_{\kappa \eta} \left( \frac{\pi}{2\kappa r} \right)^{1/2} e^{-\kappa r},$$

$$\rho = \sqrt{\eta + 1/4}. \quad (18)$$

For small  $r$ , we have

$$K_{\rho}(\kappa r) \underset{r \rightarrow 0}{\sim} \frac{\pi}{\sin(\pi \rho)} \left[ \frac{(\kappa r/2)^{-\rho}}{\Gamma(1-\rho)} - \frac{(\kappa r/2)^{\rho}}{\Gamma(1+\rho)} \right]. \quad (19)$$

One can see from Eq. (19) that for the real index,  $\rho$ , these functions diverge at  $r \rightarrow 0$  where the point dipole approximation is inadequate, so the existence (or absence) of binding electron states for  $\eta > -1/4$  when  $\rho$  is real, is determined by the behavior of the NM potential at small  $r$ .

If we consider the binding to NM caused only by its point dipole moment, then these dipole-bound states arise for  $\eta < -1/4$  when  $\rho$  is imaginary. It is easy to see that  $\eta = -1/4$  corresponds to the above cited critical value  $d = 1.625 \text{ D}$ . Assuming  $\rho = is$  in Eq. (19), we calculate the normalization factor  $N_{\kappa \eta}$  to obtain

$$R_{\kappa \eta}(r) = \left( \frac{2 \sinh \pi s}{\pi s} \right)^{1/2} \frac{\kappa}{\sqrt{r}} K_{is}(\kappa r),$$

$$s = \sqrt{|\eta| - 1/4}, \quad \eta < -1/4. \quad (20)$$

One can notice from Eq. (19) that for small  $r$  the functions  $R_{\kappa \eta}(r)$  (20) demonstrate oscillatory behavior

$$R_{\kappa\eta}(r) \underset{r \rightarrow 0}{\sim} - \frac{\kappa\sqrt{\pi}\sin[\beta_s(\kappa r)]}{|\Gamma(1+is)|\sqrt{s}\sinh\pi s}, \quad (21)$$

$$\beta_s(\kappa r) = s \ln(\kappa r/2) - \arg \Gamma(1+is), \quad (22)$$

that differs significantly from the wave functions of an electron in zero-range potential, which describes the outer electron in atomic anions [59].

Note also another interesting property of function (20): For any  $E < 0$ , they satisfy the boundary conditions imposed on bound state wave functions, i.e., their values are bounded both at  $r \rightarrow 0$  and  $r \rightarrow \infty$ , independently of  $E < 0$ . In other words a *continuous and unlimited from below spectrum of bound states* arises in the field of a point dipole with  $\eta < -1/4$ . In this sense, it is a unique case in quantum mechanics excluding a more trivial case, such as quasicontinuous spectra of bound states of an electron in a macroscopic potential box. Such behavior of bound states, so-called “fall into the center” [71], is accompanied by nonorthogonality of the wave functions corresponding to different energies.

However, this problem is interesting only from mathematical point of view, and connected with the singularity of the Sturm–Liouville problem (17) at  $r=0$ . Physically, it means that the point dipole model is not valid at small  $r \sim r_0$ , where  $r_0$  is some characteristic dimension of NM. According to general principles of quantum mechanics [71], this phenomenological MN “radius” is related to characteristic energy of the excess electron as  $E \sim \hbar^2/m_e r_0^2$  [see Eq. (24) below]. Similar parameters were introduced in various one-electron DBA models [14,19,68] to regularize the singular point dipole (or polarization) potential at small  $r$ . Such regularization can be achieved, for instance, by considering the NM as an extended dipole [7], or by taking into account some short-range repulsive core potential [9,10,43]. We use the simplest regularization model of the nonpenetrated core with the radius  $r_0$ . In practical applications,  $r_0$  is of the order of Bohr radius, and in this domain the final result is not sensitive to a particular choice of  $r_0$ .

The boundary condition in this model reads as  $R_{\kappa\eta}(r_0) = 0$ , so the bound state spectrum is expressed in terms of discrete  $\kappa_n(s)$  values determined by roots of the McDonald function:

$$K_{is}(\kappa_n(s)r_0) = 0. \quad (23)$$

For  $\kappa r_0 \ll 1$ , we can use Eq. (21) to obtain the energies of bound states:

$$E_{ns} = - \frac{\kappa_n^2(s)}{2m_e} = - \frac{2\hbar^2}{m_e r_0^2} \exp \left\{ - \frac{2\pi n}{s} + \frac{2}{s} \arg \Gamma(1+is) \right\},$$

$$n = 1, 2, \dots \quad (24)$$

Note that a formula such as Eq. (24), describes the spectrum of high-excited states of an electron for various regularizations of the dipole singularity [72–74]. Similar expression can be obtained [75] with the help of self-conjugated expansion of the operator (17) rather than using the above regularization.

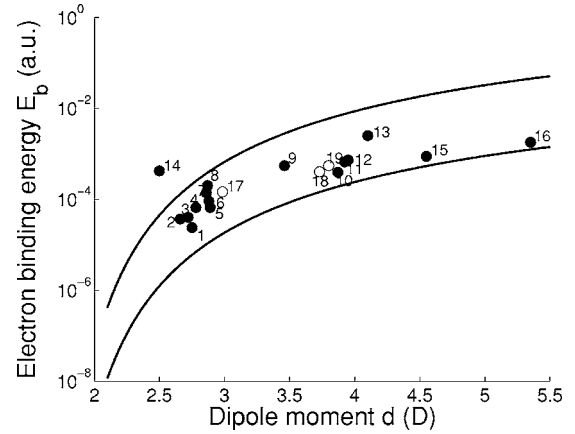


FIG. 1. Electron binding energy,  $E_b$ , as function of the dipole moment,  $d$ . Experimental (filled circles) and theoretical *ab initio* (open circles) values for Pivaldehyde (1), Butanal (2), Acetaldehyde (3), 2-Butanone (4), TFMB (5), Cyclohexanone (6), Acetone (7), Cyclobutanone (8), Metacrylonitrile (9), Acetonitrile (10), Nitromethane (11), Piridazine (12), Thymine (13), Adenine (14), Ethylene Carbonate (15), Vinylene Carbonate (16), Imidazole (17), Formamide (18), HCN (19) are taken from Ref. [15] (1)–(6) (8)–(14), (17)–(19), Ref. [76] (7), Ref. [77] (15 and 16). The curves are calculated according to Eq. (24) with  $r_0=0.5$  a.u. (upper curve) and  $r_0=3$  a.u. (lower curve).

It occurs that the expression (24) is quite accurate even for the lowest state  $n=1$  since  $\kappa_1(s)$  differs by less than 5% from the value determined by the Eq. (23) for  $0 < s < 4.58$  corresponding to  $1.625 \text{ D} < d < 35.88 \text{ D}$ .

In the Fig. 1, the expression (24) with  $n_0=1$  is compared with the experimental data. It is seen that for a number of molecules, the NM radius is limited to a reasonable range:  $r_0=0.2 \dots 2 \text{ \AA}$ .

## B. Continuum states

Radial wave functions  $R_{k\eta}(r)$  of continuum states satisfy Eq. (17) for  $E=1/2\hbar^2 k^2/m_e > 0$ . For the below-critical dipole values,  $\eta > -1/4$ , the radial function,

$$R_{k\eta}(r) = \sqrt{\frac{2\pi k}{r}} J_\rho(kr), \quad (25)$$

is proportional to the Bessel function  $J_\rho(kr)$  with the real index  $\rho = \sqrt{\eta + 1/4}$  since the second linearly independent solution,  $J_{-\rho}(kr)$ , is not regular at  $r=0$ . For the above-critical dipole values,  $\eta < -1/4$  due to the fall into center of the wave function,  $R_{k\eta}(r)$  can be an arbitrary combination of two Bessel functions  $J_{\pm is}(kr)$  of imaginary index  $is = i\sqrt{|\eta| - 1/4}$ . To fix the coefficients of such combination, one should choose a regularization of the singular dipole potential. A natural way to do it consists in choosing  $R_{k\eta}(r)$  to be  $k$  independent at small  $r \sim r_0$  [78]. Assuming  $kr_0$  to be small enough, and choosing the wave function to be real, it yields for  $\eta < -1/4$ :

$$R_{k\eta}(r) = i \frac{N_{k\eta}}{2\sqrt{r}} [\Gamma(1-is)(kr_0/2)^{is} e^{i\delta} J_{-is}(kr) - \Gamma(1+is)(kr_0/2)^{-is} e^{-i\delta} J_{is}(kr)], \quad (26)$$

$$N_{k\eta} = \frac{\sqrt{2\pi k}}{|\Gamma(1+is)|} \{\sin^2[\delta + \beta_s(kr_0)] + \sinh^2[\pi s/2]\}^{-1/2}, \quad (27)$$

where  $\beta_s(\varkappa r)$  is defined by Eq. (22) and  $\delta$  is determined by the regularization of the dipole singularity at  $r \rightarrow 0$ . For the simplest nonpenetrated core model  $R_{k\eta}(r_0)=0$ , so for  $kr_0 \ll 1$ , one easily finds  $\delta=0$ . This value is used thereafter.

The normalization of radial functions (26) is chosen to satisfy the standard condition adopted in scattering theory [71]:

$$\int_0^\infty r^2 R_{k\eta}(r) R_{k'\eta'}(r) dr = 2\pi \delta(k-k').$$

Then the asymptotic ( $r \rightarrow \infty$ ) behavior of the continuum wavefunctions is given by

$$R_{k\eta}(r) \underset{r \rightarrow \infty}{\sim} \frac{2}{r} \sin\left(kr - \frac{\pi\gamma}{2} + \frac{\pi}{4}\right),$$

$$\tan \gamma = -\tanh[\pi s/2] \tan[s \ln(kr_0)], \quad (28)$$

One can see that for the above-critical dipole  $N_{k\eta}$  in Eq. (27) demonstrates oscillatory behavior without constant limit at  $r_0 \rightarrow 0$ . The same behavior at  $k \rightarrow 0$  is responsible for the above mentioned Gailitis-Damburg oscillations [50]. At the same time, for complex wave numbers  $k=i\varkappa$ , this normalization factor

$$N_{i\varkappa\eta} = \frac{\sqrt{2\pi i\varkappa}}{|\Gamma(1+is)|} \{\sin[\beta_s(\varkappa r_0)] \sin[\beta_s(\varkappa r_0) + \pi s]\}^{-1/2} \quad (29)$$

tends to infinity exactly at the discrete spectrum points (24). This is not surprising since the wave function normalized according to the Eq. (28) is expressed in terms of the  $S$  matrix, [75] and should therefore have peculiarities at the discrete spectrum points  $k=i\varkappa_n$ .

Assuming  $k=i\varkappa$  in Eq. (26), we obtain

$$R_{i\varkappa\eta}(r) = i N_{i\varkappa\eta} \frac{|\Gamma(1+is)|}{2\sqrt{r}} \{\sin[\beta_s(\varkappa r_0)] K_{is}(-\varkappa r) - i \sin[\beta_s(\varkappa r_0) + i\pi s] K_{is}(\varkappa r)\}, \quad (30)$$

where it is easy to see that the term with  $K_{is}(-\varkappa r)$  vanishes at  $\varkappa=\varkappa_n$  since  $\beta_s(\varkappa_n r_0)=\pi n$  (24) and  $R_{i\varkappa\eta}(r)$  is proportional to the bound state wave function (20), as expected.

The wave functions of the final state with the asymptotics of ingoing (-) or outgoing (+) wave are

$$\Psi_{\mathbf{k}}^{(\pm)}(\mathbf{r}) = \sum_{\eta\lambda} A_{\mathbf{k}\eta\lambda}^{(\pm)} R_{k\eta}(r) \mathcal{Z}_{\eta\lambda}(\theta, \varphi), \quad (31)$$

with coefficients  $A_{\mathbf{k}\eta\lambda}^{(\pm)}$  chosen to satisfy the following asymptotic relation at  $r \rightarrow \infty$ :

$$\Psi_{\mathbf{k}}^{(\pm)} \approx \exp(i\mathbf{k}\mathbf{r}) + \begin{cases} f(\hat{\mathbf{k}}, \hat{\mathbf{r}}) \\ f^*(-\hat{\mathbf{k}}, \hat{\mathbf{r}}) \end{cases} \frac{\exp(\pm ikr)}{r}, \quad (32)$$

where  $\hat{\mathbf{k}}=\mathbf{k}/k$ ,  $\hat{\mathbf{r}}=\mathbf{r}/r$ . Requiring the scattering amplitude,

$$\begin{cases} f(\hat{\mathbf{k}}, \hat{\mathbf{r}}) \\ f^*(-\hat{\mathbf{k}}, \hat{\mathbf{r}}) \end{cases} = \lim_{r \rightarrow \infty} r e^{\mp ikr} [\Psi_{\mathbf{k}}^{(\pm)}(\mathbf{r}) - e^{i\mathbf{k}\mathbf{r}}],$$

to be finite at  $r \rightarrow \infty$  with the help of the standard plane wave expansion [71]

$$\exp(i\mathbf{k}\mathbf{r}) \sim \frac{4\pi}{kr} \sum_{l\lambda} i^l \sin(kr - \pi l/2) Y_{l\lambda}^*(\hat{\mathbf{k}}) Y_{l\lambda}(\hat{\mathbf{r}})$$

and the asymptotics (28) of the radial functions, one finds

$$A_{\mathbf{k}\eta\lambda}^{(\pm)} = \pm \frac{2\pi i}{k} \mathcal{Z}_{\eta, \mp\lambda}^*(\mp \hat{\mathbf{k}}) e^{\mp i(\gamma + \pi/4)} \quad (33)$$

in a way similar to that used in Ref. [63] for estimation of electron scattering on polar molecular cation, where some additions to the Rutherford formula were deduced.

#### IV. GENERAL EXPRESSIONS FOR PHOTODETACHMENT CROSS SECTION

In dipole approximation, the differential PD cross section for the electron transition from the initial state,  $|\varkappa\eta\lambda\rangle$ , to the final  $|\mathbf{k}\rangle$  state due to absorption of a photon with the frequency  $\omega$  and the unit polarization vector  $\boldsymbol{\varepsilon}$  is [79]:

$$d\sigma_{\boldsymbol{\varepsilon}}(\varkappa\eta\lambda \rightarrow \mathbf{k}; \omega) = \frac{e^2 m_e k \omega}{2\pi \hbar^2 c} |\langle \varkappa\eta\lambda | (\mathbf{r} \cdot \boldsymbol{\varepsilon}) | \mathbf{k} \rangle|^2 d\Omega_{\mathbf{k}}. \quad (34)$$

Here,  $\Omega_{\mathbf{k}}$  is the solid angle of the outgoing electron wave vector,  $\mathbf{k}$  and the dipole matrix element is

$$\langle \varkappa\eta\lambda | (\mathbf{r} \cdot \boldsymbol{\varepsilon}) | \mathbf{k} \rangle = \int R_{\varkappa\eta}(r) \mathcal{Z}_{\eta\lambda}(\hat{\mathbf{r}}) (\mathbf{r} \cdot \boldsymbol{\varepsilon}) \Psi_{\mathbf{k}}^{(-)}(\mathbf{r}) d\mathbf{r}. \quad (35)$$

For the photon polarization parallel ( $\boldsymbol{\varepsilon}=\hat{\mathbf{z}}$ ) and perpendicular ( $\boldsymbol{\varepsilon}=\hat{\mathbf{x}}, \hat{\mathbf{y}}$ ) to the dipole direction, integrating over the angular variables  $\varphi$  and  $\vartheta$  in the matrix element (35) yields

$$\langle \varkappa\eta\lambda | z | \mathbf{k} \rangle = \sum_{\eta'} A_{\mathbf{k}\eta'\lambda}^{(-)} B_{\eta\eta'}^{\lambda 0} Q(\varkappa\eta\lambda; k\eta'0),$$

$$\langle \varkappa\eta\lambda | y | \mathbf{k} \rangle = i \langle \varkappa\eta\lambda | x | \mathbf{k} \rangle,$$

$$\langle \varkappa\eta\lambda | x | \mathbf{k} \rangle = \frac{1}{\sqrt{2}} \sum_{q=\pm 1} \sum_{\eta'} A_{\mathbf{k}\eta'\lambda+q}^{(-)} B_{\eta\eta'}^{\lambda q} Q(\varkappa\eta\lambda; k\eta'_{\lambda+q}), \quad (36)$$

where

$$B_{\eta\eta'}^{\lambda q} = \sum_{l'} \left( \frac{2l'+1}{2l+1} \right)^{1/2} a_{\eta l}^{(\lambda)} a_{\eta' l'}^{(\lambda-q)} C_{l'0}^{l0} C_{l'\lambda-q}^{l\lambda},$$

$$Q(\kappa\eta_\lambda; k\eta'_{\lambda+q}) = \int_{r_0}^{\infty} r^3 R_{\kappa\eta_\lambda}(r) R_{k\eta'_{\lambda+q}}(r) dr, \quad (37)$$

with the  $\lambda$ -dependency of  $\eta$  explicitly specified. Through this dependence, the radial integral  $Q(\kappa\eta; k\eta')$  depends on the incident photon polarization.

After integration of Eq. (34) over  $d\Omega_{\mathbf{k}}$  with the help of Eqs. (33) and (36), we obtain the PD cross section for the photon polarized parallel and perpendicularly to the dipole moment correspondingly:

$$\sigma_{x,y}(\kappa\eta_\lambda; \omega) = \frac{\pi e^2 m_e \omega}{\hbar^2 k c} \sum_{\eta', q=\pm 1} |B_{\eta\eta'}^{\lambda q} Q(\kappa\eta_\lambda; k\eta'_{\lambda+q})|^2,$$

$$\sigma_z(\kappa\eta_\lambda; \omega) = \frac{2\pi e^2 m_e \omega}{\hbar^2 k c} \sum_{\eta'} |B_{\eta\eta'}^{\lambda 0} Q(\kappa\eta_\lambda; k\eta'_\lambda)|^2. \quad (38)$$

Formula (38) has a form of channel sum over partial cross sections. Each channel is characterized by  $\eta'$  value, similar to the orbital quantum number value  $l$  specifying the partial cross section in the spherically symmetric case. After averaging over the NM dipole moment, which is equivalent to chaotic orientation of DBA in the initial state, we have

$$\sigma(\kappa\eta; \omega) = \frac{1}{3} \sum_{\nu=x,y,z} \sigma_\nu(\kappa\eta; \omega). \quad (39)$$

Similar to the case of spherically symmetric systems (e.g., atoms), expression (39) does not include any dependence of the incident photon polarization [79]. However, unlike the atomic case, it includes the matrix elements of two types  $\sigma_z \neq \sigma_x = \sigma_y$ , determined by Eq. (36) and cannot be expressed through a single “reduced” matrix element.

The radial integral (37) involving wave functions (20) and (26) or (25) depends weakly on the  $r_0$  due to the  $r^3$  factor in the integrand. Thus, one can calculate the integral from  $r=0$  and use Eq. 7.7(31) of Ref. [70], Vol. 2] to express the radial integrals in terms of Gaussian hypergeometric functions:

$$Q(\kappa\eta; k\eta') = \frac{iN_{k\eta'}}{\kappa^2} \left( \frac{\sinh \pi s}{2\pi s} \right)^{1/2} [\Gamma(1-is) \times (\kappa r_0/2)^{is'} M_{is,-is'}(\omega) - (s' \leftrightarrow -s')], \quad \eta < -1/4, \quad (40)$$

$$= \frac{2}{\kappa^2} \left( \frac{k \sinh \pi s}{s} \right)^{1/2} \left( \frac{\hbar\omega}{E_b} - 1 \right)^{\rho'/2} \times M_{is,\rho'}(\omega), \quad \eta > -1/4; \quad (41)$$

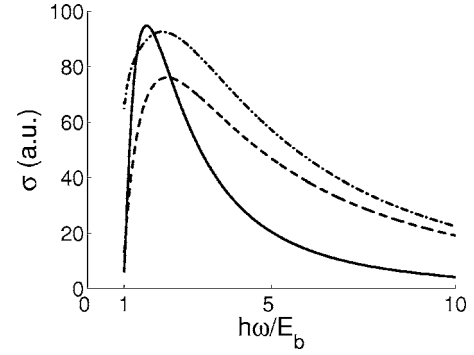


FIG. 2. Cross section of PD as function of photon frequency for different dipole moments  $d=5D$  (solid line),  $d=6D$  (dashed line), and  $d=7D$  (dashed-dotted line);  $r_0=3$  a.u.,  $E_b=11.5$  meV.

$$M_{is,\nu}(\omega) = \frac{\Gamma\left(\frac{\nu}{2} + \frac{is}{2} + \frac{3}{2}\right) \Gamma\left(\frac{\nu}{2} - \frac{is}{2} + \frac{3}{2}\right)}{\Gamma(1+\nu)} {}_2F_1\left(\frac{\nu}{2} + \frac{is}{2} + \frac{3}{2}, \frac{\nu}{2} - \frac{is}{2} + \frac{3}{2}; 1 + \nu; 1 - \frac{\hbar\omega}{E_b}\right) \quad (42)$$

$$= G_{is,\nu} \left( \frac{E_b}{\hbar\omega} \right)^{-(\nu+3-is)/2} F_1\left(\frac{\nu}{2} - \frac{is}{2} + \frac{3}{2}, \frac{\nu}{2} - \frac{is}{2} - \frac{1}{2}; 1 - is; \frac{E_b}{\hbar\omega}\right) + (s \leftrightarrow -s); \quad (43)$$

$$G_{is,\nu} = \frac{\Gamma\left(\frac{\nu}{2} - \frac{is}{2} + \frac{3}{2}\right) \Gamma(is)}{\Gamma\left(\frac{\nu}{2} + \frac{is}{2} - \frac{1}{2}\right)}. \quad (44)$$

We used the energy conservation law

$$\frac{k^2}{\kappa^2} = \frac{\hbar\omega}{E_b} - 1, \quad (45)$$

and Eqs. 2.10(3,5) of the [Ref. [70], Vol. 1.]

## V. RESULTS AND DISCUSSION

The frequency dependence of the PD cross section is presented in Fig. 2 for  $E_b=11.5$  meV and different dipole moments. The same frequency dependence for  $d=6D$  and different  $E_b$  values is given in Fig. 3. Note again that the cross section does not tend to zero at the threshold, i.e., at  $\hbar\omega/E_b=1$  (see discussion in Sec. V B).

One can see from Figs. 2 and 3 that a typical PD cross section dependence on photon frequency,  $\omega$ , has a maximum whose width decreases with an increase in  $d$  or  $E_b$ . The value,  $\sigma_m$ , of this maximum shows a complex nonmonotonic dependence on the binding energy,  $E_b$ , and the NM dipole moment,  $d$ . Some examples of such a dependence are given in Figs. 4 and 5.

Our simple analytic model agrees well, at least within the order of value, with the recent numerical calculations based

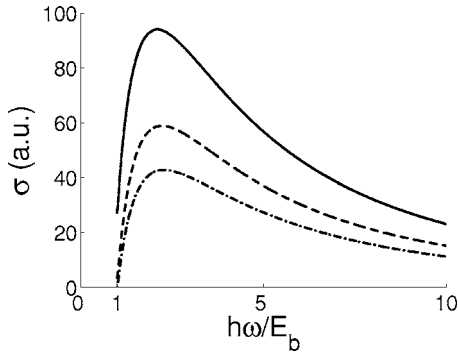


FIG. 3. Cross section of PD as function of photon frequency for different bound energies of the DBA:  $E_b=20$  meV (solid line),  $E_b=15$  meV (dashed-line),  $E_b=10$  meV (dashed-dotted line);  $r_0=3$  a.u.,  $d=6$  D.

on the Drude oscillator model [46]. The comparison with their results is given in the Figs. 6 and 7; the values of  $E_b$  and  $d$  are equal to those used in Ref. [46]. We note that our Fig. 4 is also in agreement with the  $\sigma_m \sim 1/E_b$  dependence described in Ref. [46].

As can be seen from Eq. (38), the  $\sigma(\omega)$  dependence is determined by  $Q$  factors (37) multiplied by  $(\omega/k)$ . Since the analytical expressions for  $Q$  factors (40) and (41) in terms of hypergeometric functions are quite complicated, we study two limiting cases below; high frequencies  $\omega \gg E_b/\hbar$  and threshold frequencies  $\omega \sim E_b/\hbar$ , in which both the hypergeometric functions in Eqs. (42) and (43) correspondingly have zero argument and therefore are equal to unity:

$${}_2F_1(a, b; c; z \rightarrow 0) \rightarrow 1. \quad (46)$$

It should be noted that both limits considered below are determined by the specific behavior of electron wave function in the dipole NM potential at small  $r$  (high  $\omega$ ) and large  $r$  (threshold  $\omega$ ). Therefore, these results cannot be obtained by perturbative methods (e.g., in Born approximation).

#### A. High frequencies

Consider first the below-critical dipole channels,  $\eta' > -1/4$ . Assuming  $\hbar\omega/E_b \rightarrow \infty$  in Eqs. (43) and (41) with the help of Eq. (46), we obtain

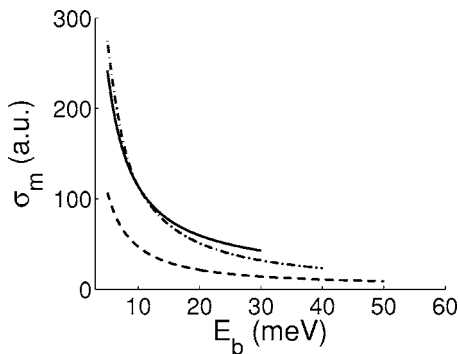


FIG. 4. Cross section maximal value,  $\sigma_m$ , as function of the binding energy,  $E_b$ , of the excess electron for different dipole moments  $d=5$  D (solid line),  $d=6$  D (dashed line), and  $d=7$  D (dashed-dotted line);  $r_0=3$  a.u.

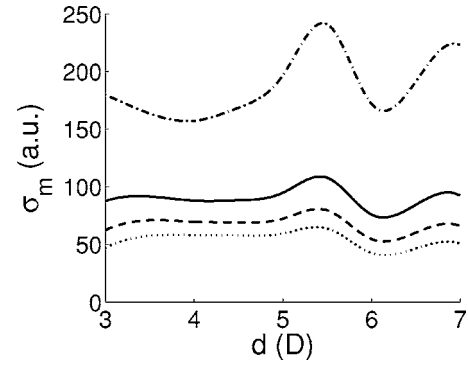


FIG. 5. Cross section maximal value,  $\sigma_m$ , as function of the NM dipole moment,  $d$ , for different binding energies  $E_b=6$  meV (dashed-dotted line),  $E_b=12$  meV (solid line),  $E_b=16$  meV (dashed line), and  $E_b=20$  meV (dotted line);  $r_0=3$  a.u.

$$Q(\chi\eta; k\eta') \underset{\omega \rightarrow \infty}{\sim} |G_{is, \rho'}| \frac{4E_b}{\chi^2 \hbar} \sqrt{\frac{k \sinh \pi s}{s}} \times \cos[s \ln \sqrt{\hbar\omega/E_b} - \arg G_{is, \rho'}]. \quad (47)$$

For the above-critical dipole channels,  $\eta' < -1/4$ , one obtains more complicated expressions of the type (47) containing several combinations of cosines with amplitudes and phases involving  $G_{\pm is, \pm is'}$ . However, one can neglect the  $\omega$ -dependence of these cosines due to a slow variation of logarithms. Then we obtain from Eq. (38), the following asymptotic behavior of PD cross section at high frequencies:

$$\sigma_{x,y,z}(\chi\eta; \omega) \underset{\omega \rightarrow \infty}{\propto} \omega^{-2}. \quad (48)$$

This dependence differs from PD cross sections in  $s$  states of atomic negative ions [ $\sigma(\omega) \sim \omega^{-3/2}$ ], but agrees with the experimental data [33] for DBA. The difference from the zero-range potential model is caused by the  $1/\sqrt{r}$  behavior of wave functions (20) in the small  $r$  domain that is different from the  $1/r$  behavior of the wave functions in the zero-range potential.

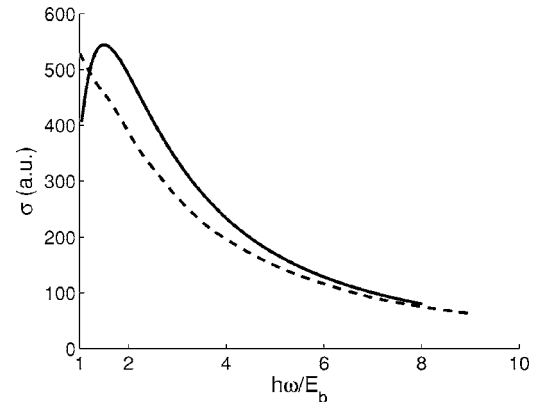


FIG. 6. Cross section of PD as a function of photon frequency for  $\text{HCN}^-$  anion: Present work (solid line) and Fig. 4(a) of Ref. [46] (dashed line).

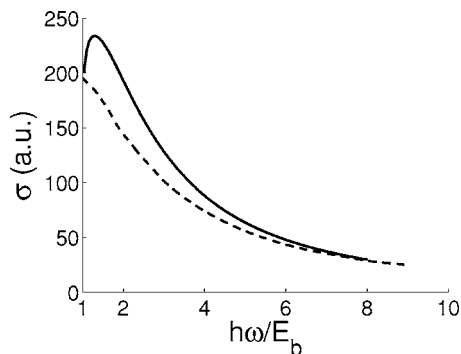


FIG. 7. Cross section of PD as a function of photon frequency for  $\text{HNC}^-$  anion: Present work (solid line) and Fig. 6(a) of Ref. [46] (dashed line).

The  $\omega^{-2}$  behavior (48) of  $\sigma(\omega)$  is obtained from  $\omega \rightarrow \infty$  limit of integral (37), where we assumed  $r_0=0$ . Since in the limit of high  $\omega \rightarrow \infty$ , the integral is determined by small  $r$  domain, asymptotics (48) is valid for not very high  $\omega$ , provided that the de Broglie wavelength of the excess electron is larger than the effective core radius:  $k \sim \sqrt{2m_e\omega/\hbar} \lesssim 1/r_0$ . Assuming  $r_0 \sim 1 \text{ \AA}$ , the frequencies  $\omega \sim 3 \text{ eV}$  used in Ref. [33] obey this condition. Actually, for higher frequencies, ionization of the inner electronic shells becomes more probable than detachment of the dipole-bound electron.

### B. Threshold behavior

At threshold frequencies, i.e., in the  $\omega \rightarrow E_b/\hbar$  (or  $k \rightarrow 0$ ) limit, our analytical expressions agree with the general threshold laws of atomic and molecular physics [47].

Since, due to relation (46), the  $M_{is,\nu}$  values in Eq. (42) are frequency-independent at the threshold, the  $\omega$  dependence of PD cross section is determined by the normalization factors of the continuum state wave functions. For the below-critical channels,  $\eta > -1/4$  from Eqs. (41), (45), and (38), one obtains

$$\sigma_{x,y,z}(\kappa\eta; \omega) \underset{\omega \rightarrow E_b/\hbar}{\propto} (\hbar\omega - E_b)^\rho, \quad (49)$$

where  $\rho$  is the minimal below-critical value of  $\rho'$  involving into the channel sum (38). Dependence (49) has a form of the Wigner law (1) at noninteger  $l$  considered for molecules in Refs. [48,49]. Note that the limit of small dipole moment  $d \rightarrow 0$  leads to a spherically symmetric, i.e., atomic potential and the eigenvalue  $\eta \rightarrow l(l+1)$  with an integer  $l$ . Then, according to Eq. (20), we have  $\rho = l + 1/2$ , and Eq. (49) is reduced to the Wigner law (1).

For the above-critical channels, oscillatory behavior of  $\sigma_{x,y,z}(\kappa\eta; \omega)$  at threshold arises due to the normalization factor (27) in a way analogous to the Gailitis-Damburg oscillations,

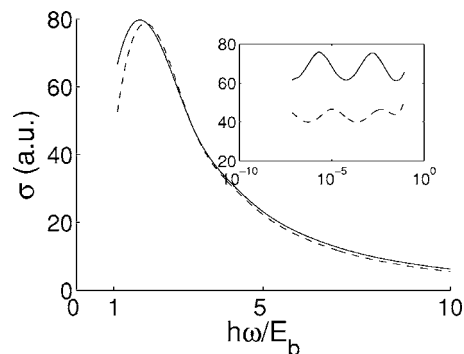


FIG. 8. Cross section of PD for acetonitrile DBA. The inset shows the Gailitis-Damburg oscillations of the cross section near threshold.  $E_b=12 \text{ meV}$ ;  $r_0=3 \text{ a.u.}$  Solid line corresponds to  $d=3.9 \text{ D}$ , dashed line corresponds to  $d=4.3 \text{ D}$

as can be seen from Fig. 8 inset. However, such non-monotonic behavior of the PD cross section near the threshold can hardly be resolved experimentally because of NM rotation [47].

Figure 8 shows the oscillating threshold behavior of the PD cross section  $\sigma_z(\omega)$  when the incident radiation is polarized along the dipole direction. For the perpendicular polarization, the cross section tends to zero at threshold according to Wigner's law, since no above-critical channels enter sum (38) for  $|\lambda| > 0$  (the first value  $\eta < -1/4$  arises for  $|\lambda|=1$  at  $d \approx 9.646 \text{ D}$ ).

### VI. CONCLUSION

We proposed the simple analytical theory for DBA with the NM modeled by the point dipole with nonpenetrating core in the BOA. Our approach gives an analytic expression (24) for binding energy of the excess electron in DBA, which is in accord with the numerical calculations reported previously [15,77]. The nonperturbative analytical theory of DBA PD was developed. For threshold frequencies of incident radiation, this theory gives the well-known Gailitis-Damburg oscillations, while for high frequencies the PD cross section demonstrates  $\omega^{-2}$  behavior in agreement with the experiment [33].

### ACKNOWLEDGMENTS

We express our gratitude to R. Compton who pointed out the problem considered here, to F. B. Dunning for his interest to our work, and to S. I. Marmo for helpful discussion. This work was partially supported by Russian Foundation of Basic Research (Grant No. 04-02-16649) and by joint BRHE Program of U. S. Civilian Research and Development Foundation and Russian Ministry of Education and Science (Grant Nos. VZ 010-0 and Y1-CP-10-04).

- [1] R. N. Compton and N. I. Hammer, in *Advances in Gas-Phase Ion Chemistry*, edited by N. Adams and I. Babcock (Elsevier Science, New York, 2001), Vol. 4, pp.257–291.
- [2] K. D. Jordan and F. Wang, *Annu. Rev. Phys. Chem.* **54**, 367 (2003).
- [3] E. Fermi and E. Teller, *Phys. Rev.* **72**, 399 (1947).
- [4] A. S. Wightman, *Phys. Rev.* **77**, 521 (1950).
- [5] R. F. Wallis, R. Herman, and H. W. Milnes, *J. Mol. Spectrosc.* **4**, 51 (1960).
- [6] M. H. Mittelman and V. P. Myerscough, *Phys. Lett.* **23**, 545 (1966).
- [7] J. M. Levy-Leblond, *Phys. Rev.* **153**, 1 (1967).
- [8] J. E. Turner, V. E. Anderson, and K. Fox, *Phys. Rev.* **174**, 81 (1968).
- [9] O. H. Crawford, *Proc. Phys. Soc. London* **91**, 279 (1967).
- [10] K. D. Jordan and W. Luken, *J. Chem. Phys.* **64**, 2760 (1976).
- [11] W. R. Garrett, *Chem. Phys. Lett.* **5**, 393 (1970).
- [12] W. R. Garrett, *Phys. Rev. A* **3**, 961 (1971).
- [13] W. R. Garrett, *J. Chem. Phys.* **77**, 3666 (1982).
- [14] C. Desfrancois, H. Abdoul-Carime, and J. P. Schermann, *Int. J. Mod. Phys. B* **12**, 1339 (1996).
- [15] H. Abdoul-Carime and C. Desfrancois, *Eur. Phys. J. D* **2**, 149 (1998).
- [16] C. D. Finch, R. A. Popple, P. Nordlander, and F. B. Dunning, *Chem. Phys. Lett.* **244**, 35 (1995).
- [17] J. M. Weber, M.-W. Ruf, and H. Hotop, *Z. Phys. D: At., Mol. Clusters* **37**, 351 (1996).
- [18] R. N. Compton, F. B. Dunning, and P. Nordlander, *Chem. Phys. Lett.* **253**, 8 (1996).
- [19] C. Desfrancois, H. Abdoul-Carime, N. Khelifa, and J. P. Schermann, *Phys. Rev. Lett.* **73**, 2436 (1994).
- [20] R. L. Jackson, A. H. Zimmerman, and J. I. Brauman, *J. Chem. Phys.* **71**, 2088 (1979).
- [21] J. Marks, J. I. Brauman, R. D. Mead, K. R. Lykke, and W. C. Lineberger, *J. Chem. Phys.* **88**, 6785 (1988).
- [22] K. Yokoyama, G. W. Leach, J. B. Kim, and W. C. Lineberger, *J. Chem. Phys.* **105**, 10696 (1993).
- [23] K. R. Lykke, R. D. Mead, and W. C. Lineberger, *Phys. Rev. Lett.* **52**, 2221 (1984).
- [24] R. D. Mead, K. R. Lykke, W. C. Lineberger, J. Marks, and J. I. Brauman, *J. Chem. Phys.* **81**, 4883 (1984).
- [25] E. A. Brinkman, S. Berger, J. Marks, and J. I. Brauman, *J. Chem. Phys.* **99**, 7586 (1993).
- [26] J. H. Hendricks, H. L. de Clercq, S. A. Lyapustina, and K. H. Bowen, *J. Chem. Phys.* **107**, 2962 (1997).
- [27] S. Y. Han, J. H. Kim, J. K. Song, and S. K. Kim, *J. Chem. Phys.* **109**, 9656 (1998).
- [28] G. H. Lee, S. T. Arnold, J. G. Eaton, and K. H. Bowen, *Chem. Phys. Lett.* **321**, 333 (2000).
- [29] M. Gutowski *et al.*, *Phys. Rev. Lett.* **88**, 143001 (2002).
- [30] R. A. Popple, C. D. Finch, and F. B. Dunning, *Chem. Phys. Lett.* **234**, 172 (1995).
- [31] R. N. Compton *et al.*, *J. Chem. Phys.* **105**, 3472 (1996).
- [32] B. A. Zon, *Appl. Phys. Lett.* **86**, 151103 (2005).
- [33] Ch. G. Bailey, C. E. H. Dessent, M. A. Johnson, and K. H. Bowen, *J. Chem. Phys.* **104**, 6976 (1996).
- [34] K. D. Jordan, K. M. Griffing, J. Kenney, E. L. Andersen, and J. Simons, *J. Chem. Phys.* **64**, 4730 (1976).
- [35] M. Gutowski, P. Skurski, A. I. Boldyrev, J. Simons, and K. D. Jordan, *Phys. Rev. A* **54**, 1906 (1996).
- [36] M. Gutowski, P. Skurski, K. D. Jordan, and J. Simons, *Int. J. Quantum Chem.* **64**, 183 (1997).
- [37] M. Gutowski, K. D. Jordan and J. Simons, *J. Phys. Chem. A* **102**, 2633 (1998).
- [38] M. Gutowski, K. D. Jordan, and P. Skurski, *J. Phys. Chem. A* **102**, 2624 (1998).
- [39] P. Skurski, M. Gutowski, and J. Simons, *J. Chem. Phys.* **110**, 274 (1999).
- [40] P. Skurski, M. Gutowski, and J. Simons, *J. Chem. Phys.* **114**, 7443 (2001).
- [41] K. A. Peterson and M. Gutowski, *J. Chem. Phys.* **116**, 3297 (2002).
- [42] A. Sawicka and P. Skurski, *Chem. Phys.* **282**, 327 (2002).
- [43] F. Wang, and K. D. Jordan, *J. Chem. Phys.* **114**, 10717 (2001).
- [44] V. E. Chernov and B. A. Zon, *Proceedings of Contributed Paper ICPEAC 2003*, Stockholm, July 2003.
- [45] L. Suess, Y. Liu, R. Parthasarathy, and F. B. Dunning, *J. Chem. Phys.* **119**, 12890 (2003).
- [46] M. Sindelka, V. Spirko, P. Jungwirth, F. Wang, S. Mahalakshmi, and K. D. Jordan, *J. Chem. Phys.* **121**, 1824 (2004).
- [47] H. R. Sadeghpour, J. L. Bohn, M. J. Cavagnero, B. D. Esryk, I. I. Fabrikant, J. H. Macek, and A. R. P. Rau, *J. Phys. B* **33**, R93 (2000).
- [48] P. C. Engelking, *Phys. Rev. A* **26**, 740 (1982).
- [49] D. R. Herrick and P. C. Engelking, *Phys. Rev. A* **29**, 2421 (1984).
- [50] M. Gaillitis and R. Damburg, *Zh. Eksp. Teor. Fiz.* **44**, 1644 (1963) [*Sov. Phys. JETP* **17**, 1107 (1963)].
- [51] Ch. H. Greene and A. R. P. Rau, *Phys. Rev. A* **32**, 1352 (1985).
- [52] C. R. Liu, N. Y. Du, and A. F. Starace, *Phys. Rev. A* **43**, 5891 (1991).
- [53] I. I. Fabrikant, *Zh. Eksp. Teor. Fiz.* **73**, 1317 (1977) [*Sov. Phys. JETP* **46**, 693 (1977)].
- [54] J. R. Smith, J. B. Kim, and W. C. Lineberger, *Phys. Rev. A* **55**, 2036 (1997).
- [55] C. Delsart, F. Goldfarb, and C. Blondel, *Phys. Rev. Lett.* **89**, 183002 (2002).
- [56] A. Osterwalder, M. J. Nee, J. Zhou, and D. M. Neumark, *J. Chem. Phys.* **121**, 6317 (2004).
- [57] F. Goldfarb, C. Drag, W. Chaibi, S. Kroger, Ch. Blondel, and Ch. Delsart, *J. Chem. Phys.* **122**, 014308 (2005).
- [58] M. Ya. Amusia, N. B. Avdonina, E. G. Drukarev, S. T. Manson, and R. H. Pratt, *Phys. Rev. Lett.* **85**, 4703 (2000).
- [59] Yu. N. Demkov and V. N. Ostrovsky, *Zero-Range Potentials and their Applications in Atomic Physics*, (Plenum, New York, 1988).
- [60] B. A. Zon, *Phys. Lett. A* **203**, 373 (1995); *Laser Phys.* **7**, 806 (1997).
- [61] U. Fano, *Phys. Rev. A* **2**, 353 (1970); Ch. Greene and Ch. Jungen, *Adv. At. Mol. Phys.* **21**, 51 (1985).
- [62] P. Debye, *Polar Molecules* (Chemical Catalog Co., New York, 1929).
- [63] B. A. Zon, *Zh. Eksp. Teor. Fiz.* **102**, 36 (1992) [*Sov. Phys. JETP* **75**, 19 (1992)].
- [64] J. K. G. Watson, *Mol. Phys.* **81**, 227 (1994).
- [65] P. G. Alcheev, V. E. Chernov, and B. A. Zon, *J. Mol. Spectrosc.* **211**, 71 (2002).
- [66] P. G. Alcheev, R. J. Buenker, V. E. Chernov, and B. A. Zon, *J. Mol. Spectrosc.* **218**, 190 (2003).

- [67] V. E. Chernov, I. Yu. Kiyani, H. Helm, and B. A. Zon, *Phys. Rev. A* **71**, 033410 (2005).
- [68] D. C. Clary, *J. Phys. Chem.* **92**, 3173 (1988).
- [69] J. Simons, *J. Chem. Phys.* **91**, 6858 (1989).
- [70] *Higher Transcendental Functions*, edited by H. Bateman and A. Erdelyi, (McGraw-Hill, New York, 1953).
- [71] L. D. Landau and E. M. Lifshitz, *Quantum Mechanics (Non relativistic Theory)*, (Pergamon, Oxford, 1977).
- [72] G. F. Drukarev, *Electron Collisions with Atoms and Molecules*, (Moscow, Nauka, 1978) (in Russian).
- [73] U. Fano and A. R. P. Rau, *Atomic Collisions and Spectra* (Academic, New York, 1986).
- [74] M. J. Moritz, Ch. Eltschka, and H. Friedrich, *Phys. Rev. A* **63**, 042102 (2001).
- [75] A. I. Baz', Ya. B. Zel'dovich, and A. M. Perelomov, *Scattering, Reactions and Decay in Nonrelativistic Quantum Mechanics* (Israel Program for Scientific Translations, Jerusalem, 1969).
- [76] N. I. Hammer, R. N. Compton, L. Adamowicz, and S. G. Stepanian, *Phys. Rev. Lett.* **94**, 153004 (2005).
- [77] N. I. Hammer, R. J. Hind, R. N. Compton, K. Diri, K. D. Jordan, D. Radisic, S. T. Stokes, and K. H. Bowen *J. Chem. Phys.* **120**, 685 (2003).
- [78] T. F. O'Malley, *Phys. Rev.* **137**, A1668 (1965).
- [79] I. I. Sobelman, *Atomic Spectra and Radiative Transitions* (Springer, Berlin, 1979) (Russ. original, *PhysMathLit*, Moscow, 1963).